Rare Earth Elements in Acid Mine Drainage

/Carlos Ayora *(1)*, Francisco Macías *(2)*, Ester Torres *(1)*, José Miguel Nieto *(2)*

(1) Instituto de Diagnóstico Ambiental y Estudios del Agua, CSIC, c/ Jordi Girona 18, 08034 Barcelona
(2) Departamento de Geología, Universidad de Huelva, Av. Fuerzas Armadas s/n, 21071 Huelva

Abstract

Rare Earth Elements and Yttrium (REY) are raw materials of increasing importance for modern technological developments. Most of production is concentrated in China, and finding alternative sources of REY has become a need for the rest of countries. Acid Mine Drainage (AMD) may contain REY in concentration various orders of magnitude higher than the rest of waters. The distribution pattern of AMD is depleted in light (and less expensive) REE with respect to the clay standards. REY does not segregate into Fe(III) precipitates in acidic streams. Mixing with more alkaline streams increases pH above 5, and REY are entirely scavenged from solution with basaluminite. The same behaviour is observed in calcite based passive remediation systems of AMD. There, schwertmannite precipitates do not allocate REY that are completely retained in the basaluminite precipitation front. No change in the distribution pattern is observed in this retention process. Although REY rates in the basaluminite treatment residue are competitive, the annual reserves are far below those targeted by current prospecting. However, AMD is expected to run for hundreds of years and therefore, total reserves are unlimited.

Key-words: *acid rock leaching, passive remediation, basaluminite, Iberian Pyrite Belt*

1. Introduction

Rare Earth Elements (REE) together with yttrium (REY) are essential raw materials for modern technological applications. Their most important uses include the manufacturing of permanent magnets for wind turbines, alloys for rechargeable batteries and jet engines, and phosphor light-emitting compounds for plasma, liquid crystals or light emitting diodes. The REE group is arbitrarily divided into light (LREE: La to Nd), medium (MREE: Sm to Gd) and heavy (HREE: Tb to Lu); due to it atomic size similarity, Y is often considered with HREE. On the other hand, this division has important economic implications, because HREE and MREE are priced higher than LREE (most traded REE are Eu, Tm and Lu).

In 2011, global demand was 105 kt of REY oxides and is expected to grow up to 160 kt in 2016 (Hatch, 2012). Most of REY mined deposits are located in carbonatites and other alkaline magmatic intrusive rocks. These rocks are localized in stable continental cratons and crystalline blocks of old Earth crust controlled by intracontinental rift and fault systems (Berger et al., 2009). Additional resources of REY are found adsorbed on clays deposits from weathering and reworking of original primary igneous rocks. China controls the world production of REY, in the last decade the Chinese production reached 97%. The Bayan Obo super large carbonatites deposit currently accounts for some 90% of the REE production, whereas the rest of production (accounting for 6-7%) comes from ion-adsorption clays deposits (Kinicky et al., 2012). Bayan Obo carbonatite is mainly rich in LREE, whereas clays are richer in HREE. On the other hand, REE have been traditionally used in Geosciences as geochemical tracers since several decades ago. The similar atomic structure and chemical properties of the REE group support their very similar geochemical behaviour through many geological processes. However, the small chemical differences among the elements of the group also enable their use to identify processes such as redox, differential sorption, etc. In such tracer studies, rather than comparing the absolute values, the relative enrichment pattern of the different

Depósito legal: CA-602-2004 / ISSN: 1698-5478

REE with respect to a reference material has been the main target of research. Thus, chondrite is commonly used as a reference of an undifferentiated planetary material in igneous petrogenesis. For Earth surface processes, such as weathering, paedogenesis and hydrochemistry, the REE concentration in a pool of clays (Post-Archaen Australian Shales PAAS, and/or North American Shale Composite NASC, *McLennan, 1989)* is currently used as reference.

The present paper aims to review and summarize the REY content in Acid Mine Drainage (AMD), considering both the total amount and the relative enrichment pattern of the different elements. In order to complete the REY cycle, novel data on their behaviour in AMD neutralization and treatment is also described.

2. REY Behaviour and Concentration in AMD Environments

Noack et al. (2014) present a comprehensive study of distribution of REE in groundwater, lakes, rivers and oceans. According to these authors the REE concentration in natural waters, with a dispersion of one to two orders of magnitude, shows medians around 5, 53, 71, 170 pmol/L for ocean, groundwater, rivers and lakes, respectively.

On the other hand, a strong correlation between high concentration of REE and acidity has been reported both in surface and ground waters, as well as in leaching studies of soils with different pH solutions (*Noack et al., 2014; Welch et al., 2009; Fernandez-Caliani et al., 2009*). Thus, the REE contents reported in AMDs (*Merten et al. 2005; Welch et al., 2009; Da Silva et al., 2009; Sahoo et al., 2012; Borrego et al, 2012*; our unpublished data) show a range between 4,000 and 80,000 pmol/L, clearly several orders of magnitude above the medians of natural waters (*Fig. 1*).

The reasons for the REE enrichment in AMD with respect to the rest of natural waters are grounded in their aqueous geochemistry. A minor part of REE in rocks is concentrated in accessory minerals, such as zircon, monacite or allanite (Chakhmouradian and Wall, 2012). These minerals do not undergo weathering, and therefore they concentrate in detrital rocks and placers. However, the majority of REE in igneous and sedimentary rocks are occasionally located as major components of carbonates (bastnaesite) and phosphates (monazite), and more commonly as traces in rock forming silicates, such as plagioclase. Weathering of these minerals in conventional soils occurs due to the aggressive action of CO_2 and humic acids. Once in solution, REE in soil pore water remain as trivalent cations or, at neutral to alkaline pH complexed with CO_3^{2-} and OH- (*Fig. 2A*). Due to its large positive charge and ionic potential, trivalent cations are strongly sorbed onto the negative charged surface of clays, kaolinite and illite, or replace Na and Ca in the interlayer positions of smectites (*Bradbury and Baeyens, 2002; 2009; Coppin et al., 2002; Tertre et al., 2005*). As a consequence, REE are mainly concentrated in clays, which become a major reservoir of REE in sedimentary rocks. If the primary rock is rich in REE, weathering clays may become an economical target for mining, such as the residual deposits in South China (*Kynicky et al., 2012*).

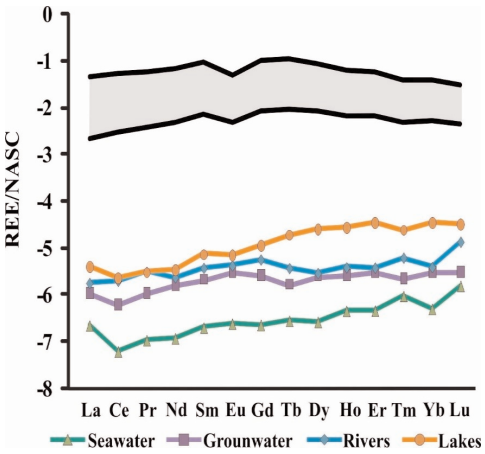

Fig. 1. NASC normalized REE diagram for natural waters (average from Noack et al., 2014), and for reported and unpublished data of AMDs (shaded area).

However, in AMD systems the dissolution of Fe sulfides generates acidic solutions with much lower pH. The dissolution rate of alumi-

nosilicates increases with the catalitic action of H^+ (*Bloom and Stilling, 1995*), and, therefore, dissolution of rocks and the release of solutes to the pore water are much more intense in AMD environments than in the rest of weathering profiles. Once in solution, REE are mostly complexed forming $REESO_4^+$, which is the dominant complex in AMD waters (*Fig. 2B*). Sulfate complexation inhibits the sorption of REE in clays and stabilizes them in the solution. As a consequence of the intense rock attack and the formation of stable complexes in solution, AMD contain REE concentrations much higher than other natural waters (Figures 1 and 3).

Redox changes merely affect Eu and Ce in AMD, the only lanthanides which exhibit two different oxidation states. Divalent Eu is only stable at negative Eh (<-0.3 V) and near neutral pH, conditions only reached at the bottom of lakes and estuaries. On the contrary, Ce^{4+} occurs at oxidizing and neutral-alkaline waters, and the precipitation of CeO_2 is probably responsible for the depleted Ce concentration is seawater (*McLennan, 1989*).

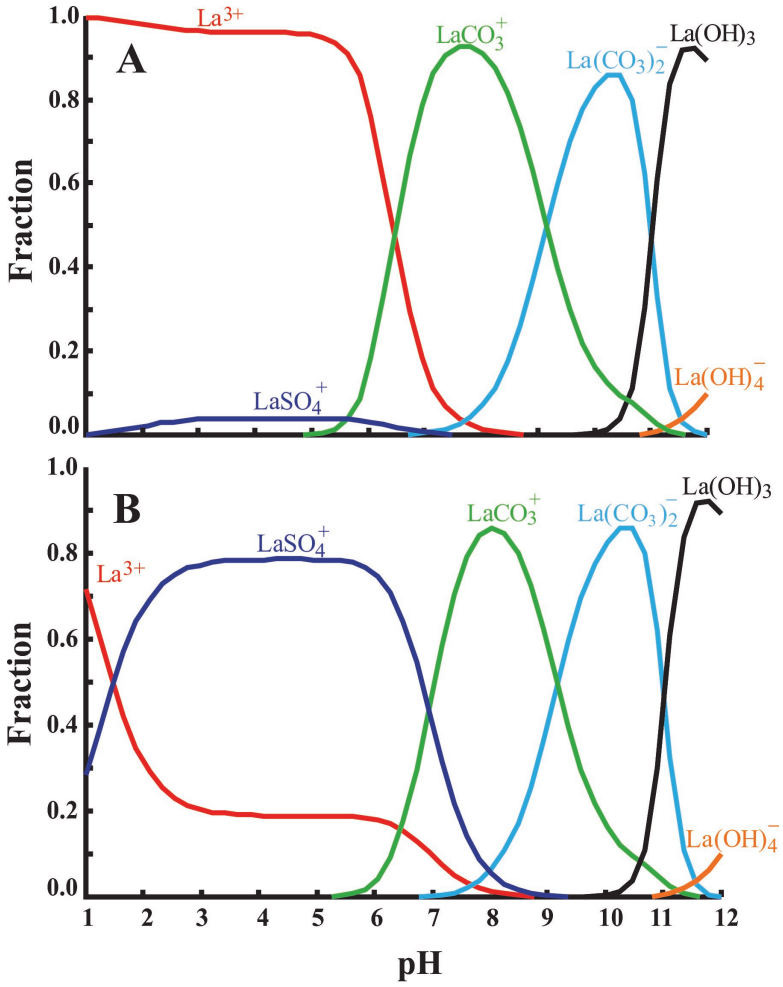

Fig. 2. Variation of the relative abundance of La^{3+} aqueous species with pH in: A) pore water of a regular weathering profile ([Total Inorganic Carbon]= 1 mM; [SO4]= 0.01 mM]; B) acid mine water ([Total Inorganic Carbon]= 0.01 mM; [SO4]= 1 mM]). Thermodynamic data from MEDUSA database (Puig-Domenech, 2010).

Depósito legal: CA-602-2004 / ISSN: 1698-5478

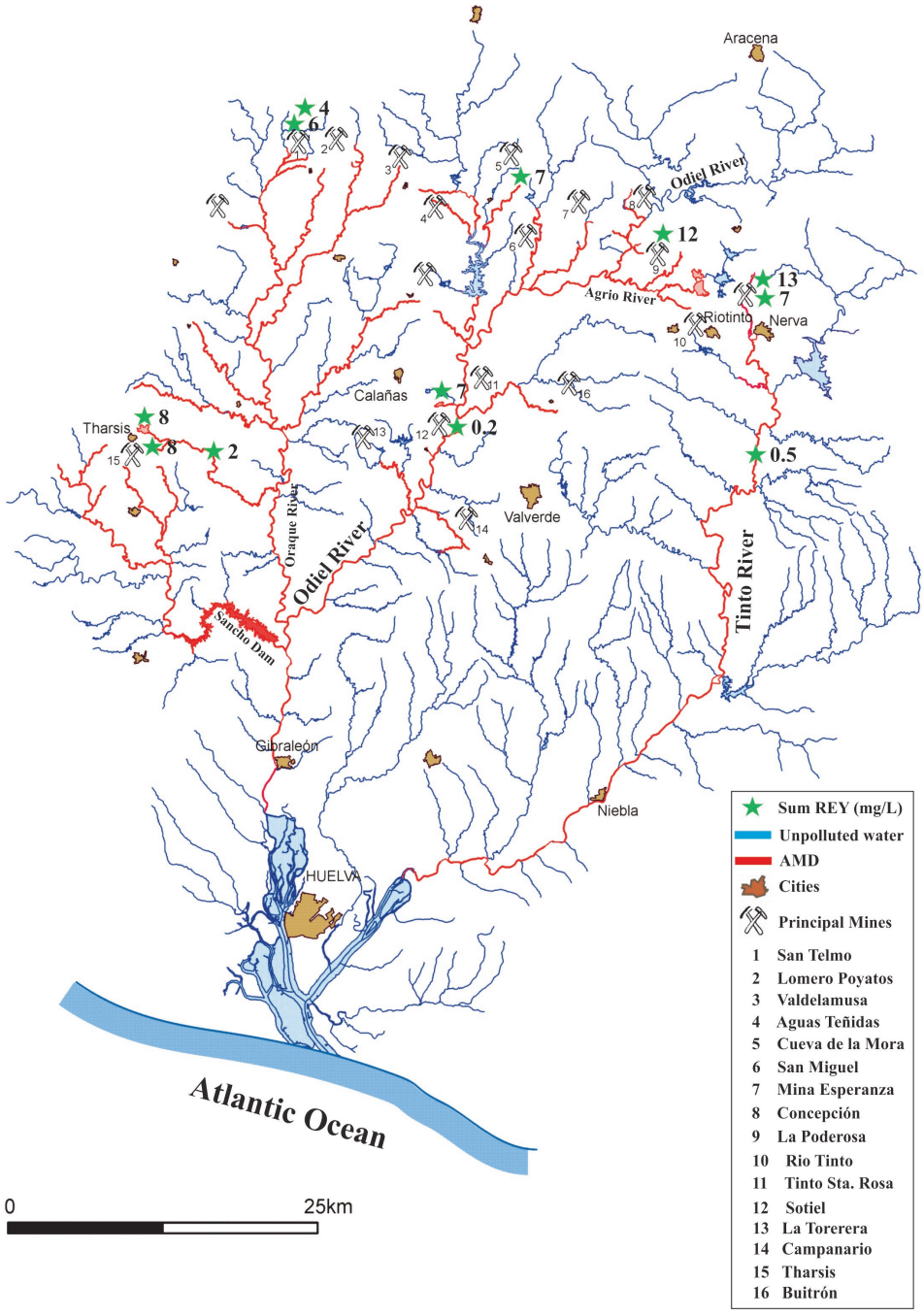

Fig. 3. Concentration of REY (mg/L) of some AMD in the Tinto and Odiel basins (SW Spain).

Beyond their total amount, the REE distribution pattern in AMD is distinctly different from that in the rest of surface and groundwater (*Fig. 1*). The NASC-normalized REE spectra of ocean and continental waters show a relative enrichment in HREE. This is attributed to the formation of progressively stronger carbonated complexes in solution with increasing atomic number, which inhibits HREE sorption compared with LREE (*Johannesson et al., 1999).*

On the contrary, the NASC-normalized REE patterns in AMD show a typical convex curvature (*Figure 1 and 4*) indicating an enrichment in MREE with respect to LREE and HREE (da *Silva et al., 2009; Perez-Lopez et al., 2010; Sahoo et al., 2012*). This distinct REE distribution in AMD is not completely explained, although it seems to be controlled by the Fe cycle. Thus, NASC-normalized REE distributions of pyrite ore bodies and clay soil matrices are practically flat, with a negative Eu anomaly. *Welch et al. (2009)* show a strong enrichment of LREE in jarosite, and their counterpart depletion in pore water of acid sulfate soils. This enrichment is consistent with the MREE-depleted pattern shown by the gossan resulting from supergene alteration of sulfide deposits (*Fig. 4*). In some cases, the subsequent transformation of jarosite to goethite releases some LREE to porewater, resulting in a distribution enriched in MREE but asymmetric, relatively enriched in LREE compared to HREE (*Welch et al., 2009*).

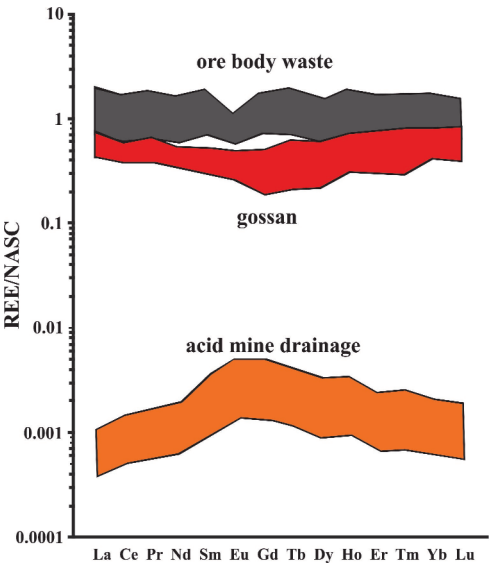

Fig. 4. NASC normalized patterns of disseminated ore wastes, gossan and AMD's from Sao Domingos mine area, Portugal (modified from Pérez-López et al., 2010)

Rare earth elements geochemistry in AMD solutions is strongly linked to pH, and therefore to AMD neutralization processes. *Verplanck et al.(2004)* describe that REEs behave conservatively in two acidic streams at pH below 5.1, and partitioned into the solid phases at pH between 5.1 and 6.1. These authors also confirmed these observations by neutralization of six AMD solutions in the laboratory. Similarly, *Wood et al. (2006)* also reported the preferential partition of HREE over LREE into the solid phase as pH increased above 6 in two watersheds impacted by AMD and by volcanic discharges. This is also consistent with the decrease in REE observed downstream the confluence of an AMD with a tributary and the pH increase from 3 to 6 in Lousal mine, Portugal (*da Silva et al., 2009*).

The processes that control the REE partitioning from aqueous to solid phase could be the precipitation of REE-bearing phases and/or sorption onto Fe and Al precipitates. Although water is supersaturated in some trace minerals, such as phosphates, they have never been detected in previous studies (*Gammons et al., 2005*). Therefore, most authors point to sorption as the process accounting for REE scavenging from AMD (*Verplanck et al., 2004; Gammons et al., 2005*). In spite of its key geochemical role, no experimental sorption studies of REE into schwertmannite and basaluminite have been carried out up to now.

When AMD effluents mix with neutral waters of receiving water bodies (*e.g. see Fig. 5*) and the pH increases accordingly, the concentrations of REE are greatly depleted in these mixing zones. In cases, mixing of AMD-impacted rivers, such as Tinto and Odiel, with seawater in the estuary also decreases their concentration. Aluminum, Fe and REE transported by the acidic rivers are extensively remo-

Depósito legal: CA-602-2004 / ISSN: 1698-5478

ved in the estuary where the acidic water is neutralized. The REE removal is due to several simultaneous mechanisms: co-precipitation with oxyhydroxides (mainly Al but also Fe), complexation with flocculating humic substances, and sorption to suspended particles (*Astrom et al., 2012*). With respect to the distribution pattern, the mixture shows a flat pattern, with the typical depletion in LREE of marine waters (*Borrego et al., 2012*). Despite of the mixing, and the lower REE concentrations, the typical MREE enriched pattern of AMD is still recognizable in the estuarine sediments of the Guadiana River, suggesting the forensic possibilities of the REE patterns in AMD impacted sediments (*Delgado et al., 2012*).

3. REY Behaviour in AMD Passive Remediation Systems

In recent decades, passive remediation systems have been implemented to treat acid drainages from coal mines. Among them, constructed wetlands with an organic substrate to support bacterially mediated sulfate reduction are the most commonly used (*Walton-Day, 1999*). Due to the high land demand of wetlands, other more compact designs, mainly based on the neutralization of acidity by means of limestone dissolution, have been developed (*Hedin et al., 1994; Rees et al., 2001; Younger et al., 2002; Cravotta, 2003; Ziemkiewcz et al., 2003; Watzlaf et al., 2004*).

These systems have been extended to metal-rich and high acidity drainages from massive sulfide mines by means of the Disperse Alkaline Substrate approach (*Rotting et al., 2008a, Ayora et al., 2013*). It consists of a fine-grained alkaline reagent (commonly limestone) mixed with an inert, coarse high-surface material (typically wood shavings), so that the surfaces of the inert matrix are partially covered with the reactive substance. The small grain size of the alkaline material provides a greater reactive surface than the

Fig. 5. Schwertmannite (red) and basaluminite (white) precipitates at the mixing zone of Odiel river (left) and the Agrio tributary (right).

same amount of coarse material, and therefore increases the dissolution rate. Also, a larger fraction of each grain can potentially be dissolved before the precipitate coatings become too thick and prevent further dissolution. This increases the proportion of reactive efficiently consumed. The inert matrix provides large pores and high permeability and separate individual reactive grains, so that precipitates do not fill the entire pore space between grains, retarding clogging problems. In some cases, additional alkalinity to precipitate divalent metals is added by the dissolution of caustic magnesia (*Rötting et al., 2006, 2008b; Macías et al., 2012a*).

From the observations on REE behaviour in rivers described above, it is expectable that an increase in pH above 5.5 will lead to the removal of REE form solution. Therefore, REE from acidic solutions can be accumulated in the precipitates of remediation systems once these pH values are reached. Therefore, the behaviour of REY in a multi-stage sequential treatment of AMD must be checked: how much amount is retired from solution in each step? In which solid phases are co-precipitated? Are they differently accumulated? To answer these questions, AMD from Cueva de la Mora mine (*Fig. 3*) was sequentially treated with column experiments of calcite and caustic magnesia during four months. Both aqueous and solid phases were be analysed.

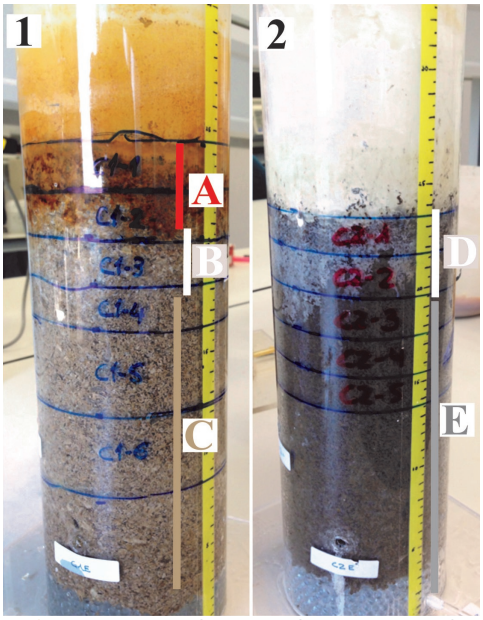

Fig. 6. Treatment columns after 4 month of AMD percolation. 1) Calcite-DAS column showing three zones: a red zone of schwertmannite (A), a white zone of basaluminite (B), and a creamy zone of gypsum and unreacted calcite (C). 2) MgO-DAS column showing a white zone of gypsum and Zn-hydroxides (D) and unreacted MgO (E).

The experimental setup is based on a downward gravitational flow; it is made up of two successive columns filled with calcite (designing to precipitate trivalent metals, *Fig. 6-1*) and caustic magnesia (for divalent metals precipitation, *Fig. 6-2)*, and decantation vessels. Physico-chemical parameters at representative points along the experimental set were obtained once a week. Samples were collected monthly, and were filtered, acidulated and refrigerated until analysis. Concentration of dissolved major and trace elements were analysed by ICP-OES and ICP-MS. Once completed the experiment, samples of the newly-formed phases were obtained in both columns and the decantation vessel. Samples were analyzed for major and trace components, and their mineralogy were studied by X-Ray Diffraction and Scanning Electron Microscope (SEM) and Energy Dispersive Spectrometry (EDS).

As already described in previous AMD treatments with calcite-DAS reactive mixture (*Rotting et al., 2008a,b; Caraballo et al.,2011a,b*), three main zones were visually distinguished in the first column (Figure 6-1). From the input downstream these zones are: a red zone characterized by the precipitation of schwertmannite; a white zone characterized by basaluminite formation, and a grey zone made up of gypsum and calcite remaining from the original reactive. After two decantation vessels, the solutions were treated with a MgO-DAS mixture (*Fig. 6-2*). A white precipitate of gypsum and complex Zn-hydroxides is formed close to the water input, with MgO remaining in the rest of the column.

Depth profiles of the calcite-DAS column, and the first cm of MgO-DAS column after four months of functioning are presented in Figure 7. The pH values ranged normally between 2.5 and 3 at the inlet, and between 5.5 and 6 at the outlet. The pH increase occurred from the beginning of the column until 10 cm in depth,

Depósito legal: CA-602-2004 / ISSN: 1698-5478

suggesting that calcite has not been consumed in the rest of the column. The pH in the decantation vessel rose to around 6.3 due to CO_2 degassing. Downstream, pH increased to 9.2 in the first 4 cm of MgO-DAS column. Finally, due to aragonite precipitation, pH decreased to 6.8 (not represented in *Fig. 7*).

Dissolved Fe in the inflow water was mostly found as Fe(III), and most of it was precipitated near the substrate surface. Aluminium precipitated at greater depth than Fe(III). Thus, the majority of Al was removed in the first 10 cm of column. Calcium concentrations displayed similar trends as pH, showing that acid neutralization was due to limestone dissolution. Calcium increased mostly in the depth interval where Al and Fe removal was highest, indicating that calcite dissolution was directly linked to Al- and Fe-hydrolysis and -precipitation. As expected, Mg concentration was constant throughout the calcite-DAS columns, and increased by 50% in the MgO-DAS column.

The depth profiles show a complete depletion in REY concentration along the treatment line. The first decrease coincided with the Al precipitation front. Thus, about 20% of REY was captured by the Al-rich solid phase. Then, a second depletion occurred along the transit through the unreacted calcite section of the column, around 15%. A final removal of 55% REY took place in the decantation vessel. Finally, the remaining 10% REY was removed in the first cm of the MgO-DAS column Among the rest of trace elements analysed, only Cu show a removal pattern very similar to REY (Fig. 7).

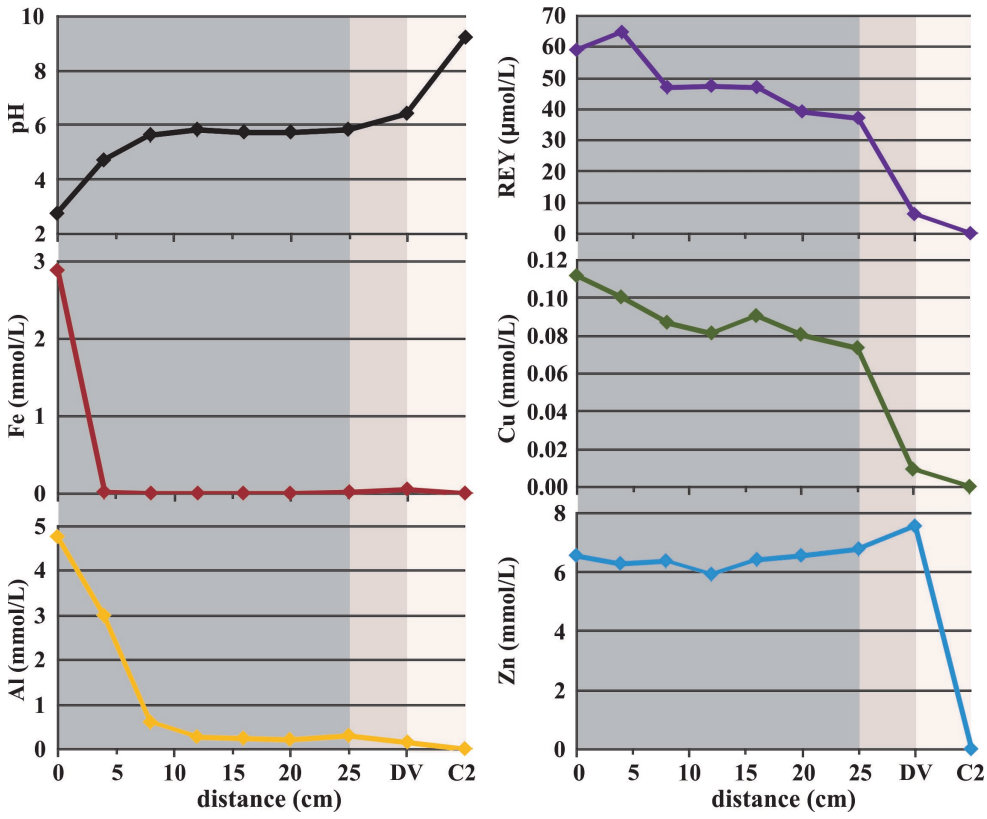

Fig. 7. Depth profiles of pH and aqueous concentrations of Al, Cu, Fe, Zn, and REY. The numbers indicate the distance to the calcite column water-solid interface, DV is the decantation vessel and C2 the first 4 cm of the MgO column

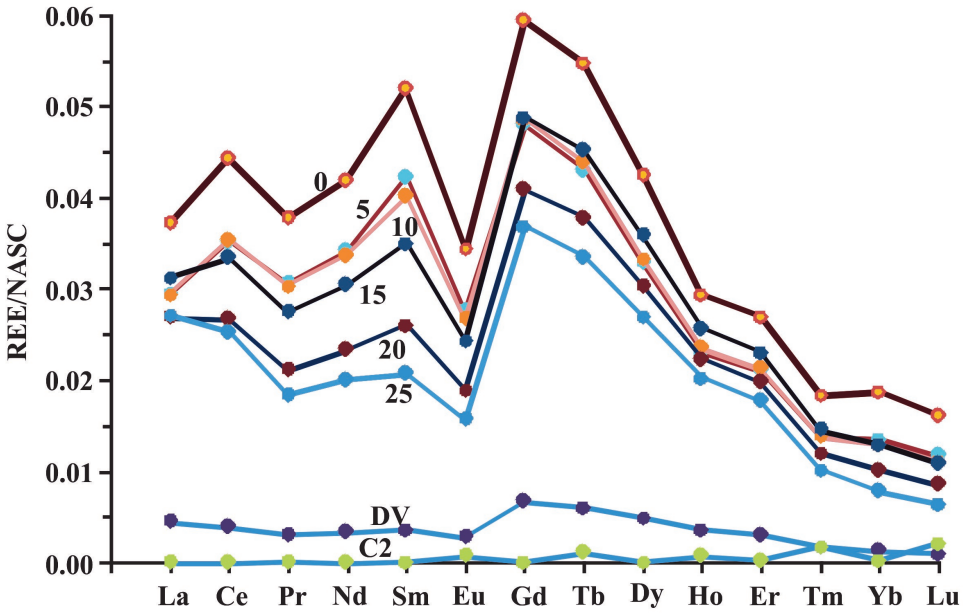

Fig. 8. REE pattern of the Cueva de la Mora AMD through the calcite and MgO treatments. The numbers indicate the distance to the calcite column water-solid interface, DV is the decantation vessel and C2 the first 4 cm of the MgO column.

Similarly than previous experiences (*Rötting et al., 2008a; Caraballo et al., 2011a,b; Macías et al., 2012a*); Zn, Mn, Cd, Co and Ni did not change in concentration in the calcite-DAS, but were completely removed in the first cms of the MgO-DAS step. Sulfate concentration did not significantly change throughout the calcite and MgO-DAS columns.

Another interesting issue is the possible fractionation of the different REE along the different removal processes. As most AMD samples (see *Fig. 1 and 4*), the inflow water showed enrichment in middle REE with a negative Eu anomaly, with respect to NASC. As shown in *Fig. 8*, the different REE showed no preferential depletion in any term along the different stages of treatment.

The main chemistry and mineralogy of solid phase samples confirms the results obtained in previous studies of DAS-treatment (*Rötting et al., 2006; Caraballo et al., 2011a,b)*, and therefore will not be discussed in detail. From the inflow water downstream, a schematic distribution of zones is: red, white, grey, decantation vessel and MgO zone, with transitional compositions in between. Schwertmannite is the mineral phase responsible for most of the iron removed in the red layer. Goethite is also found as aging product of schwertmannite. As induced from their constant concentration in pore water, no significant amounts of Cu, Zn and REY were retained in schwertmannite. This is perfectly consistent with the observations of *Verplanck et al. (2004)*, who described that REE behave conservatively in streams waters at pH below 5.1. This leads to a relevant practical consequence: REY do not disperse into schwertmannite precipitates along the streams or in a pre-treatment step developed to oxidize and precipitate Fe (*Macías et al., 2012b*) before the AMD is treated by DAS technology, and therefore, they can be entirely recovered in the DAS-treatment system.

Only gypsum and calcite were detected by XRD in the white layer and no evidence of any crystalline or poorly crystalline Al-phase was observed. The fact that a large amount of Al was removed from solution in this level suggests that some poorly ordered or amorphous Al-phases must be present. This hypothesis is also supported by SEM-EDS observations

Depósito legal: CA-602-2004 / ISSN: 1698-5478

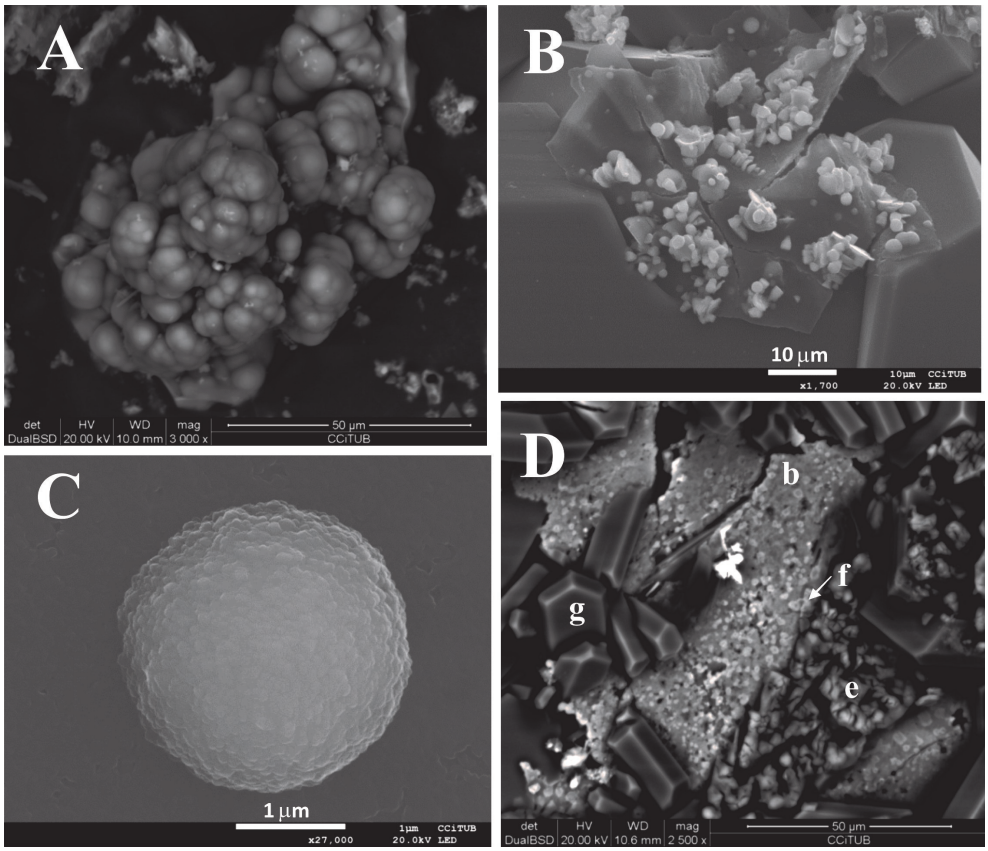

Fig. 9. Scanning Electron Microscope observation of precipitates from the calcite column treating the Cueva de la Mora AMD: A) basaluminite aggregate; B) bechererite, $(Zn,Cu)_6Zn_2(OH)_{13}[(Si,S)(O,OH)4]_2$ aggregates of monoclinic crystals together with fluorite spheres on gypsum; C) detail of a fluorite spherical aggregate; D) crystals of gypsum (g), massive precipitate of bechererite (b), fluorite (white inclusions, f) and epsomite (e) from the decantation vessel.

(*Fig. 9A*), where gypsum and an Al-hydroxysulfate appear to be closely precipitated around calcite grains. The first decrease in REY concentration occurred concomitant with Al removal. No data on REY sorption in basaluminite is available in the literature. However, *Yang et al. (2013)* described that the sorption of Eu(III) in γ–-Al2O3 depends on pH, being minimum at pH<4 and maximum at pH>8. Moreover, the preferential REE removal from different types of soils by 1M HCl solutions observed in BCR sequential extractions (*Rao et al., 2010*) is also consistent with its accumulation in Al-hydroxides similar to basaluminite. Also Cu in solution experienced a decrease with Al. The adsorption of Cu in basaluminite has been also described in the AMD's from the Thuringian slate mining area (*Rhotenhofer et al., 2000*). These authors described that around 40% of Cu was retained in Al precipitates when an AMD mixed with neutral tributaries. Similar to our column experiments, no other divalent metals were retained.

The Cu and REY concentration in pore water continued to decrease after Al was practically absent, suggesting that another mechanism of retention was occurring. Indeed, XRD and SEM-EDS observations show massive precipitation of gypsum in the decantation vessel and in the first 4 cm of the MgO-DAS columns. Together with gypsum, aggregates of trigonal crystals of bechererite, $(Zn,Cu)_6Zn_2(OH)_{13}$ $[(Si,S)(O,OH)_4]_2$, are ubiquitously found in the column (*Fig. 9B*), and

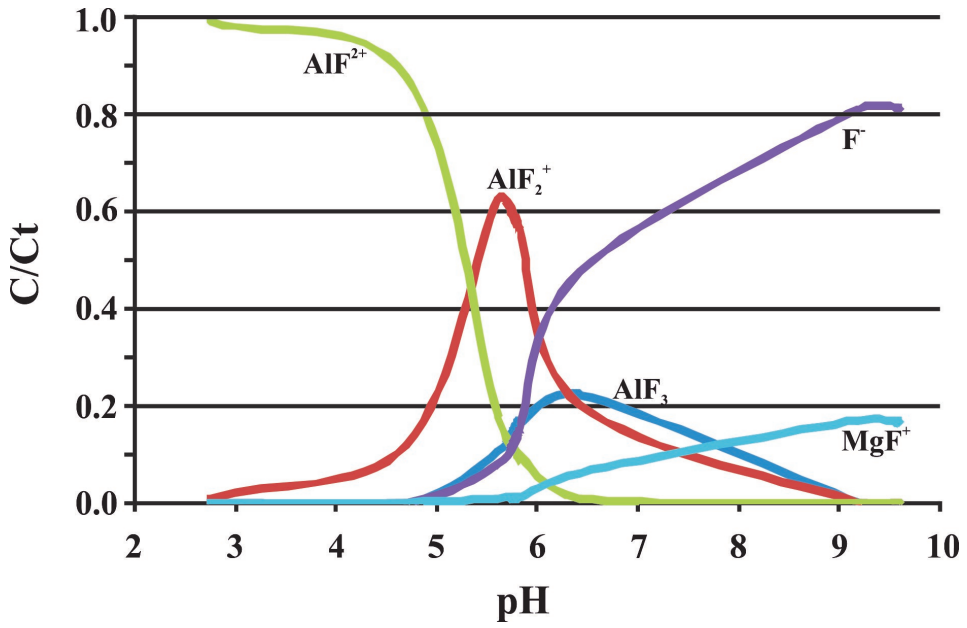

Fig. 10. Distribution of fluorine aqueous species with pH along the treatment of Cueva de la Mora AMD.

have been identified with XRD in all the samples. This mineral can account for Cu depletion in pore water. Together with bechererite, small cubes and spherical aggregates of cubic crystals of fluorite have also been observed (*Fig. 9C*). Gypsum, bechererite and fluorite were also found, together with epsomite, as massive aggregates in the bottom of the decantation vessel (*Fig. 9D*). Their formation was probably promoted by evaporation of part of the water in the vessel. Evaporation took place as indicated by the increase in Li concentration in the vessel from 46 to 70 ppb. Fluorite has also been identified by XRD in one sample of the decantation vessel. A peak of Y was distinguishable in some fluorite X-ray Energy Dispersive Spectra.

Fluorite has been investigated as a host for REE in magmatic and hydrothermal deposits. Thus, fluorite veins have been selected as a possible target for REE exploration in Australia (*Jaireth et al., 2014*), China (*Deng et al., 2014*), USA (*Pingitore et al., 2014*) and South Africa (*Graupner et al., 2015*). However, to the authors' knowledge, no REE-fluorite formation has been described at environmental temperature. The precipitation of fluorite in Cueva de la Mora experimental treatment is most probably due to a double cause. Dissolution of calcite supplies Ca^{2+} required for fluorite formation. However, no fluorite is found in the schwertmannite zone, where active dissolution of calcite is occurring. Indeed, in AMD, F- is entirely complex with Al^{3+} as AlF^{2+}. When Al is precipitated as basaluminite, the complex becomes unstable and F is mainly found as free anion F-, therefore, the saturation index of fluorite is reached and the mineral precipitates (*Fig. 10*).

4. The Iberian Pyrite Belt (IPB): a Region-scale Heap leaching for REY

More than one hundred AMD sources have been described in the Odiel and Tinto basins, both draining the IPB. They are mainly discharges from galleries and open pits, and leachates from waste dumps (Sanchez-España et al., 2005; Sarmiento, 2006). The recorded flows are very variable from 0.1 to more than 100 L/s. Moreover, according to a Mediterranean climate, the flow from a particular AMD may be also multiplied by 3 to 5 from the dry (June to November) to the rainy season (December to May).

 Depósito legal: CA-602-2004 / ISSN: 1698-5478

There is little information on the REY content in the AMDs of the IPB. Up to now, previous studies in the IPB were devoted to the role of REY as a tracer of weathering processes (*Astrom et al., 2010; da Silva et al., 2009; Pérez-López et al., 2010; Delgado et al., 2012*). The REY concentrations described in these studies vary within a wide range reaching 3.8 mg/L in some cases. An ongoing survey of REY concentrations in 35 AMD locations from IPB reveals a wide range of variation from 0.07 to 13 mg/L, with an average of 2.3 mg/L of total REY.

On the other hand, laboratory column experiments indicate two important features: 1) No REY partition between AMD and the Fe(III)-precipitates (schwertmannite and goethite) occurs. This means that REY is not partially loosed during the AMD transit in streams or pre-treatments steps, and all dissolved inventory reaches the remediation system. 2) REY can be completely retained in the basaluminite layer and the decantation residues of the calcite-DAS passive remediation systems. Therefore, REY content from AMD can be entirely recovered. Two full scale treatment systems are been building at Mina Esperanza and Mina Concepción sites (*Fig. 3*), but only one has been working for 22 months until the calcite reactive was exhausted (*Caraballo et al., 2011a,b*). The full scale system reproduced the same zonation pattern described for the columns experiment: schwertmannite, basaluminite and calcite-gypsum zones (*Fig. 11*). Unfortunately, no systematic analyses of REY were carried out. However, a first approach to annual tonnage and rate can be calculated from the total dissolved Al and REY concentration in AMD and the molar volume of basaluminite. An example for Mina Esperanza can be found in *Table 1*.

Over 100 AMD sites, with discharges varying from 1 to 100 L/s in the dry season, are known in the Odiel and Tinto Basins. Thus, about 1 m3/s can be estimated as a total AMD discharge to the two rivers in the dry season. As a rough calculation, assuming an average concentration of 2.3 mg/L of total REY, total reserves of 80 t

Fig. 11. A) View of the Mina Esperanza passive remediation systems after 22 months of functioning. B) Detail of the vertical zonation: 1) calcite-gypsum; 2) basaluminite; 3) schwertmannite zones.

Table 1.
Calculated annual tons and rate of REY in basaluminite from Mina Esperanza AMD.

	Q (L/s)	Al (mg/L)	REY (mg/L)	t Al/y	t bas/y	t REY/y	t REY2/O3	rate %
AMD	1	148.1	0.9	4.67	20.08	0.03	0.04	0.17

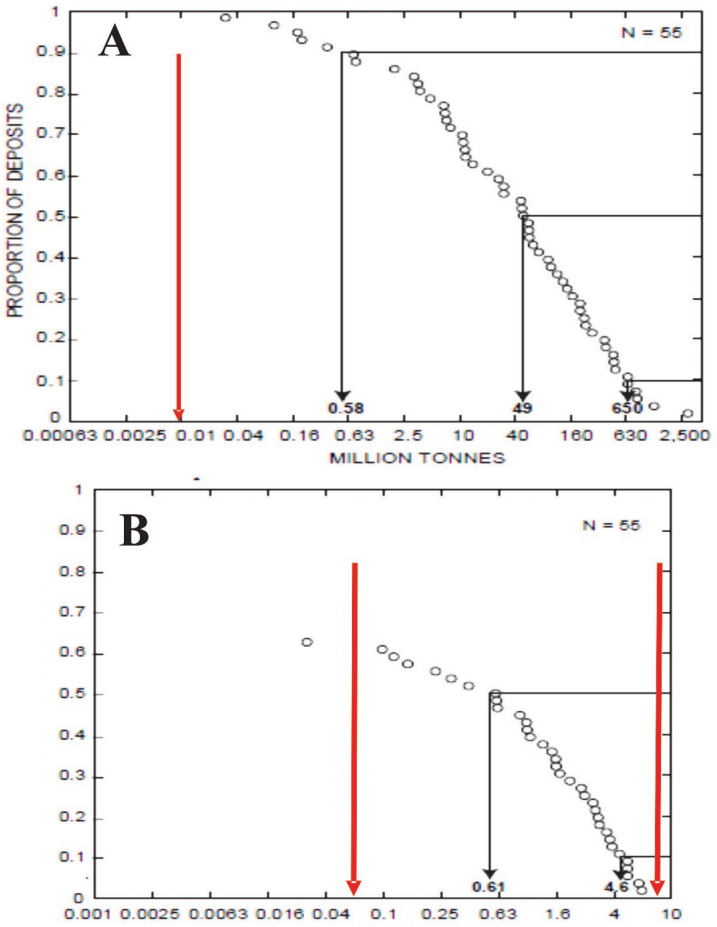

Fig. 12. Accumulative frequency of reserves (A) and mining rates (B) from conventional REY deposits (Berger et al., 2009). Red arrows indicate the REE richer and poorer AMD monitored up to now.

REY/year (100 t REY_2O_3/year) can be estimated. This annual inventory can be drastically varied as the knowledge on discharges and concentrations improves. These annual accumulation of REY is very small compared with the annual reserves of the ore deposits currently mined or explored (*Fig. 12A*). Taking into account the Al concentration recorded in the literature from the IPB (*Sanchez-España et al., 2005*), the little data available on REY concentrations, and assuming that 100% of the REY will be concentrated in basaluminite, the REY rates in these precipitates would range between 0.03 and 8% REY_2O_3 (*Fig. 12B*). These rates are similar to those of currently investigated deposits (*Fig. 12B*). However, although the annual reserves are two orders of magnitude lower than current targets of exploration, the natural processes which generate AMD are expected to continue for centuries or thousands of years () with no energy investment, therefore this issue could be considered as a renewable resource of REY.

5. Acknowledgements

The work has been funded by the CGL2013-48460-C2, CTM2014-61221-JIN, LIFE-ETAD ENV/ES/000250 and AMDREY-ERAMIN projects.

6. References

Astrom M.E., Nystrand M., Gustafson J.P., Osterholm P., Nordmyr L., Reynolds J.K. and Peltola P.(2010) Lanthanoid behaviour in an acidic landscape. Geochimica et Cosmochimica Acta74: 829–845

Astrom M.E., Osterholm P., Gustafson J.P. Nystrand M., Peltola P., Nordmyr L.andBoman A. (2012) Attenuation of rare earth elements in a boreal estuary. Geochimica et Cosmochimica Acta 96: 105–119

Ayora C., Caraballo M.A., Macías F., Rötting T.S., Carrera J. and Nieto J.M. (2013). Acid mine drainage in the Iberian Pyrite Belt: 2. Lessons learned from recent passive remediation experiences. Environmental Science and Pollution Research, 20: 7837-7853.

Berger V.I., Singer D.A. and Orris G.J. (2009). Carbonatites of the World: explored deposits of Nb and REY. Database and grade and tonnage models. USGS Open-File Report 2009-1139.

Blum E.E. and Stillings L.L. (1995) Feldspar dissolution kinetics. In A.F. White and S.L. Brantley (Eds): Chemical weathering rates of silicate minerals. Reviews in Mineralogy, 31: 291-352.

Borrego J., Carro B., Lopez-Gonzalez N., de la Rosa J., Grande J.A., Gomez T and de la Torre M.L. (2012) Effect of acid mine drainage on disolved rare earth elements geochemistry long a fluvial-estuarine system: the Tinto-Odiel Estuary (SW Spain). Hydrology Research, 43: 262-274

Bradbury M.H. and Baeyens B. (2002) Sorption of Eu on Na- and Ca-montmorillonites: Experimental investigations and modelling with cation exchange and surface complexation. Geochimica et Cosmochimica Acta, 66: 2325-2334

Caraballo M.A, Macías F., Rötting T.S., Nieto J.M. and Ayora C. (2011a) Long term remediation of highly polluted acid mine drainage: a sustainable approach to restore the environmental quality of the Odiel river basin. Environmental Pollution, 159, 3613–3619.

Caraballo M.A., Macías F., Castillo J., Quispe D., Nieto J.M. and Ayora C. (2011b) Hydrochemical performance and mineralogical evolution of a dispersed alkaline substrate (DAS) remediating the highly polluted acid mine drainage in the full scale passive treatment of Mina Esperanza (SW, Spain). American Mineralogist, 96: 1270–1277.

Chakhmouradian A.R. and Wall F. (2012) Rare Earth Elements: Minerals, Mines, Magnets (and More). Elements, 8: 333–340

Cravotta C.A. (2003) Size and performance of anoxic limestone drains to neutralize acidic mine drainage. Journal of Environmental Quality, 32, 1277–1289.

Coppin F., Berger G., Bauer A., Castet S. and Loubet M. (2002) Sorption of lanthanides on smectite and kaolinite. Chemical Geology, 182: 57-68

Da Silva E., Ferreira E. , Bobos I, Matos J., Patinha C., Reis A.P., Fonseca E.C. (2009) Mineralogy and geochemistry of trace metals and REE in massive volcanic sulphide host rocks, stream sediments, stream waters and acid mine drainage from the Lousal mine area (Iberian Pyrite Belt, Portugal). Applied geochemistry, 24: 383-401

Delgado J., Pérez-López R., Galván L., Nieto J.M. and Boski T. (2012).Enrichment of rare earth elements as environmental tracers of contamination by acid mine drainage in salt marshes: A new perspective. Marine Pollution Bulletin, 64: 1799-1808.

Deng X.H., Chen Y.J., Yao J.M., Bagas L. and Tang H.S. (2014) Fluorite REE-Y (REY) geochemistry of the ca. 850Ma Tumen molybdenite–fluorite deposit, eastern Qinling, China: Constraints on ore genesis. Ore Geology Reviews, 63: 532–543

Fernandez-Caliani J.C., Barba-Brioso C. and de la Rosa J.D. (2009) Mobility and speciation of rare earth elements in acid minesoils and geochemical implications for river waters in the southern Iberian margin. Geoderma, 149: 393-401

Gammons C.H., Wood S.A., Pedrozo F., Varekamp J.C., Nelson B.J., Shope C.L. and Baffico G. (2005) Hydrogeochemistry and rare earth element behaviour in a volcanically acidified watershed in Patagonia, Argentina. Chemical Geology 222: 249– 267

Graupner T. , Mühlbach C. , Schwarz-SchamperaU., Henjes-Kunst F., Melcher F. and Terblanche H. (2015)

Mineralogy of high-field-strength elements (Y, Nb, REE) in the world-class Vergenoeg fluorite deposit, South Africa. Ore Geology Reviews, 64: 583–601

Hatch G.P. (2012) Dynamics in the Global Market for Rare Earths. Elements, 8: 341-346

Hedin R.S., Watzlaf G.R., Nairn R.W. (1994) Passive treatment of acid-mine drainage with limestone. Journal of Environmental Quality, 23, 1338–1345.

Jaireth S.,Hoatson D.M. and Yanis M. (2014) Geological setting and resources of the major rare-earth-element deposits in Australia. Ore Geology Reviews, 62: 72-128

Johannesson K.H., Farnham I.M., Guo C. and Stetzenbach K.J. (1999) Rare earth element fractionation and concentration variations along a groundwater flow path within a shallow, basin-fill aquifer, southern Nevada, USA. Geochimica et Cosmochimica Acta, 63: 2697-2708

Kynicky J., Smith M.P. and Xu C. (2012) Diversity of Rare Earth Deposits: The Key Example of China. Elements, 8: 361–367

Macías, F, Caraballo, M.A., Rötting, T.S., Pérez-López R., Nieto J.M. and Ayora, C., (2012a).From highly polluted Zn-rich acid mine drainage to non-metallic waters: Implementation of a multi-step alkaline passive treatment system to remediate metal pollution. Science of the Total Environment 433, 323-330.

Macías, F, Caraballo, M.A., Nieto J.M., Rötting, T.S. and Ayora, C., (2012b). Natural pretreatment and passive remediation of highly polluted acid mine drainage. Journal of Environmental Management. 104, 93-100.

MacLennan S.M. (1989) Rare Earth Elements in sedimentary rocks: Influence of provenance and sedimentary processes. In B.R. Lipin and G.A. McKay (eds.): "Geochemistry and Mineralogy of Rare Earth Elements", Reviews in Mineralogy, 11:169-200.

Merten D.; Geletneky J., Bergman H., Haferburg G., Kothe E. and Büchel G. (2005) Rare Earth patterns: A tool for understanding processes in remediation of acid mine drainage. Chemie der Erde, 65: 97-114

Noack C.W, DzombakD.A. and Karamalidis A.K. (2014) Rare Earth Element Distributions and Trends in Natural Waters with a Focus on Groundwater. Environmental Science and Technology, 48, 4317_4326

Pérez-López R., Delgado J., Nieto J.M. and Márquez-García B. (2010).Rare earth element geochemistry of sulphide weathering in the São Domingos mine area (Iberian Pyrite Belt): A proxy for fluid-rock interaction and ancient mining pollution. Chemical Geology, 276: 29-40.

Pingitore N.; Clague, J. and Gorski D. (2014) Round Top Mountain rhyolite (Texas, USA), a massive, unique Y-bearing-fluorite-hosted heavy rare earth element (HREE) deposit. Journal of Rare Earths 32: 90-96

Puig-Domenech I. (2010) MEDUSA: Making Equilibrium Diagrams Using Sophisticated Algorithms. http://www.kemi.kth.se/medusa

Rao, C.R.M.,Sahuquillo A. andLopez-Sanchez J.F. (2010) Comparison of single and sequential extraction procedures for the study of rare earth elements remobilisation in different types of soils. Analytica Chimica Acta, 662: 128-136

Rees B., Bowell R., Dey M. and Williams K. (2001) Passive treatment: A walk away solution?, Mining Environmental Management, 21, 7-8.

Rothenhofer P., Sahin H. and Peiffer S. (2000) Attenuation of heavy metals and sulfate by aluminium precipitates in acid mine drainage? Acta Hydrochimica et Hydobiologica, 28: 136-144.

Rötting T.S., Cama J., Ayora C., Cortina J.L. and De Pablo J. (2006) Use of caustic magnesia to remove cadmium, nickel, and cobalt from water in passive treatment systems: Column experiments. Environmental Science & Technology, 40, 6438–6443

Rötting T.S., Thomas R.C., Ayora C. and Carrera J. (2008a) Passive Treatment of Acid Mine Drainage with High Metal Concentrations Using Dispersed Alkaline Substrate. Journal of Environmental Quality, 37, 1741–1751.

Rötting T.S., Ayora C. and Carrera J. (2008b) Improved passive treatment of high Zn and Mn con-

centrations using caustic magnesia (MgO): particle size effects. Environmental Science & Technology, 42, 9370–9377.

Sahoo P.K., Tripathy S.,Equeeniddin S.M. and Panigrahi M.K. (2012) Geochemical characteristics of coal mine discharge vis-à-vis behaviour of rare earth elements at Jaintia Hills coalfield, northeastern India. Journal of Geochemical Exploration, 112: 235-246

Sanchez-España, J., Lopez-Pamo E, Santofimia E., Aduvire O., Reyes J. and Barettino D. (2005) Acid mine drainage in the Iberian Pyrite Belt (Odiel river watershed, Huelva, SW Spain): geochemistry, mineralogy and environmental implications. Applied Geochemistry, 20: 1320-1356.

Sarmiento AM, Nieto JM, Olías M, Cánovas CR. (2009) Hydrochemical characteristics and seasonal influence on the pollution by acid mine drainage in the Odiel river Basin (SW Spain). Applied Geochemistry 24:697–714.

Tertre E., Castet S., Berger G., Loubet M. and Giffaut E. (2005) Experimental sorption of Ni2+, Cs+ and Ln3+ onto a montmorillnite up to 150 C. Geochimica et Cosmochimica Acta, 69: 4937-4948

Verplanck P.L., Nordstrom D.k. Taylor H.E. and Kimball B.A. (2004) Rare earth element partitioning between hydrous ferricoxides and acid mine water during iron oxidation. Applied Geochemistry 19 (2004) 1339–1354

Walton-Day K. (1999) Geochemistry of the processes that attenuate acid mine drainage in wetlands. In Plumlee GS, Logsdon MJ (eds): The Environmental Geochemistry of Mineral Deposits. Part A: Processes, Techniques and Health Issues. Reviews in Economic Geology Volume 6A, pp. 215-228, Society of Economic Geologists, Inc., Colorado, USA.

Watzlaf G.R., Schroeder K.T., Kleinmann R.L.P., Kairies C.L. &Nairn R.W. (2004) The passive treatment of coal mine drainage. Laboratoryreport DOE/NETL-2004/1202, U.S. Department of Energy, National Energy Technology Laboratory, Pittsburgh, PA.

Welch S.A., Christy A.G., Isaacson L and Kirste D. (2009) Mineralogical control of rare earth elements in acid sulfate soils. Geochimica et Cosmochimica Acta, 73: 44-64

Wood S.A., Gammons C.H. and Parker S.R. (2006) The behaviour of rare earth elements in naturally and anthropogenically acidified waters. Journal of Alloys and Compounds 418: 161–165

Yang S., Sheng G., Montavon G., Guo Z., Tan X., Grambow B. and Wang X. (2013)Investigation of Eu(III) immobilization on c-Al2O3 surfaces by combining batch technique and EXAFS analyses: Roleof contact time and humic acid. Geochimica et Cosmochimica Acta 121 (2013) 84–104

Younger P.L. (1997) The longevity of minewater pollution: a basis for decision-making. Science of Total Environment, 194-195: 457-466.

Younger P.L., Banwart S.A. and Hedin R.S. (2002) Mine Water: Hydrology, Pollution, Remediation. Kluwer Acad. Press, Dordrecht.

Ziemkiewicz P.F., Skousen J.G. and Simmons J. (2003) Long-term performance of passive acid mine drainage treatment systems. Mine Water Environment, 22: 118–129